J|A|C|S
ARTICLES
Published on Web 04/06/2006

Measurement of Long-Range $^{1}H-^{19}F$ Scalar Coupling Constants and Their Glycosidic Torsion Dependence in 5-Fluoropyrimidine-Substituted RNA

Mirko Hennig,*,§ Markéta L. Munzarová,† Wolfgang Bermel,‡ Lincoln G. Scott,§ Vladimír Sklenář,† and James R. Williamson§

Contribution from the Department of Molecular Biology and The Skaggs Institute of Chemical Biology, The Scripps Research Institute, MB 33, 10550 North Torrey Pines Road, La Jolla, California 92037, National Centre for Biomolecular Research, Masaryk University, Kotlarska 2, 611 37 Brno, Czech Republic, and Bruker Biospin GmbH, Rheinstetten, Germany

Received January 9, 2006; E-mail: mirko@scripps.edu

Abstract: Long-range scalar ^{5}J(H1′,F) couplings were observed in 5-fluoropyrimidine-substituted RNA. We developed a novel $S^{3}E$-^{19}F-α,β-edited NOESY experiment for quantitation of these long-range scalar ^{5}J(H1′,F) couplings, where the *J*-couplings can be extracted from inspection of intraresidual (H1′,H6) NOE cross-peaks. Quantum chemical calculations were exploited to investigate the relation between scalar couplings and conformations around the glycosidic bond in oligonucleotides. The theoretical dependence of the observed ^{5}J(H1′,F) couplings on the torsion angle χ can be described by a generalized Karplus relationship. The corresponding density functional theory (DFT) analysis is outlined. Additional NMR experiments facilitating the resonance assignments of 5-fluoropyrimidine-substituted RNAs are described, and chemical shift changes due to altered shielding in the presence of fluorine-19 (^{19}F) are presented.

Introduction

Fluorine-19 (^{19}F) NMR can provide a wealth of information about local environment, geometry, dynamical properties, and three-dimensional structure of nucleic acids. The lack of natural abundance in bioorganic and biological systems in combination with its favorable NMR properties makes ^{19}F-labeling an attractive alternative to routinely used NMR studies with other spin $I = {}^{1}/_{2}$ isotopes, such as ^{13}C, ^{15}N, and ^{31}P.[1] Fluorine-19 offers a high gyromagnetic ratio, second only to ^{1}H, providing 83% of the proton NMR sensitivity. The ^{19}F chemical shift is exquisitely sensitive to changes in the local environment largely due to an anisotropic distribution of electrons in the three 2p orbitals. At the same time, the van der Waals radius of fluorine is 1.35 Å as compared to 1.2 Å for hydrogen, which contributes a minor steric perturbation.

The magnitude and sign of scalar *J*-coupling interactions report on local bond geometries. In particular, long-range scalar ^{n}J(I,S) couplings (nuclei I and S separated by more than three bonds) provide information on the geometric arrangement of the coupled spins I and S and are largest and most frequently observed when ^{19}F is involved.[2] The observation of an intraresidual long-range scalar coupling between a fluorine nucleus covalently bound to the base C5 carbon and the anomeric H1′ proton in pyrimidine nucleosides has been previously described.[3,4] Here, we show that the magnitude of this five-bond scalar ^{5}J(H1′,F) coupling depends on the glycosidic torsion angle χ which defines the orientation of nucleobases with respect to the sugar moiety. In the *anti* conformation, the base is pointing away from the sugar available for base pairing interactions, and in the *syn* orientation, it eclipses the sugar moiety.

The experimental long-range scalar coupling data obtained in this work have been augmented by results of theoretical ab initio calculations of ^{5}J(H1′,F) couplings as a function of glycosidic torsion angle χ in the modified ribonucleosides 5-fluorouridine (5F-U) and 5-fluorocytidine (5F-C). The applied theoretical approach, by means of using models with known and adjustable geometrical parameters, enables a simple determination of the torsion angle dependence of scalar couplings. Whereas spin−spin couplings over more than three bonds have been computed previously,[5,6] to the best of our knowledge, this study represents the first ab initio treatment of the dependence of the long-range coupling on a torsion angle.

The present study was stimulated by the observation of cross-peaks connecting ^{19}F nuclei covalently bound to the base C5 carbon and anomeric H1′ protons in heteronuclear multiple bond correlations (HMBC) for 5-fluoropyrimidine-substituted RNA. Direct methods employed previously to extract the correspond-

§ The Scripps Research Institute.
† Masaryk University.
‡ Bruker Biospin GmbH.

(1) Rastinejad, F.; Evilia, C.; Lu, P. *Methods Enzymol.* **1995**, *261*, 560−575.
(2) Gakh, Y. G.; Gakh, A. A.; Gronenborn, A. M. *Magn. Reson. Chem.* **2000**, *38*, 551−558.
(3) Cushley, R. J.; Wempen, I.; Fox, J. J. *J. Am. Chem. Soc.* **1968**, *90*, 709−715.
(4) Alderfer, J. L.; Loomis, R. E.; Sharma, M.; Hazel, G. *Prog. Clin. Biol. Res.* **1985**, *172A*, 249−261.
(5) Malkin, V. G.; Malkina, O. L.; Eriksson, L. A.; Salahub, D. R. In *Theoretical and Computational Chemistry*, 2nd ed.; Seminario, J. M., Politzer, P., Eds.; Elsevier: Amsterdam, New York, 1995; pp 273−347.
(6) Barone, V.; Peralta, J. E.; Contreras, R. H.; Snyder, J. P. *J. Phys. Chem. A* **2002**, *106*, 5607−5612.

ing long-range coupling constants failed in our case because the magnitudes of the coupling were smaller than the natural line width in macromolecules. Exclusive correlation spectroscopy (E. COSY) provides an elegant way to measure scalar ^nJ(I,S) couplings especially in cases where the line width of correlated nuclei exceeds the *J*-coupling to be extracted.[7−9] Pioneering work by Sørensen and co-workers demonstrated that conventional E. COSY-type cross-peaks can be further simplified by subspectral editing according to passive spins adopting either the α or β state.[10,11]

In combination with a ^{1}H,^{1}H NOESY mixing scheme, we applied a ^{1}H,^{19}F spin state selective excitation (S^{3}E) pulse sequence element to separate the two doublet components of an E. COSY cross-peak, allowing for the measurement of long-range scalar ^5J(H1′,F) couplings in 5-fluoropyrimidine-substituted RNA. Conceptually similar experiments for the measurement of scalar and dipolar *J*(H,F) coupling interactions in RNA specifically labeled with ^{19}F at the 2′-ribose position were introduced by Luy and Marino.[12,13] In addition, we demonstrate that the ^5J(H1′,F) couplings can be readily exploited for intraresidual magnetization transfer between the ^{19}F nuclei and anomeric H1′ protons using gradient-selected HMBC experiment.[14,15] The correlations observed tremendously facilitate chemical shift assignments in 5-fluoropyrimidine-substituted RNA. In contrast, a commonly used heteronuclear ^{1}H−^{19}F NOE experiment (HOESY) becomes less sensitive at higher magnetic fields due to faster relaxation dominated by ^{19}F chemical shift anisotropy (CSA). Moreover, correlations to distant ribose protons in HOESY experiments are usually poorly resolved.[16,17]

The efficacy of these experiments was demonstrated on the 30 nucleotide human immunodeficiency virus (HIV)-2 transactivation response element (TAR) RNA uniformly labeled with either 5F-Ura or 5F-Cyt. The HIV Tat (transcription activator)−TAR complex formation provides an essential transcription regulatory function for HIV. The lentiviral protein Tat binds an RNA hairpin known as TAR (transcription activator response element) located at the 5′-end of nascent viral transcripts and thereby enhances the inefficient elongation of transcription complexes initiated at the HIV promoter. Only when Tat is bound to TAR is cellular RNA polymerase II (RNAP II) able to transcribe the entire viral RNA.[18]

Experimental Section

RNA Synthesis. 5-Fluoropyrimidine-substituted TAR RNA was synthesized by in vitro transcription reactions with bacteriophage T7 RNA polymerase according to published methods.[19,20] A detailed description of the enzymatic synthesis of 5-fluorouridine-5′-triphosphate (5F-UTP) and 5-fluorocytidine-5′-triphosphate (5F-CTP) for NMR studies will be published elsewhere. The fluorinated 5′-triphosphate analogues are readily incorporated by T7 RNA polymerase into RNA transcripts indistinguishable from that of UTP and CTP, respectively.

The purified RNA samples were concentrated and desalted using Centricon concentrators with 3 kDa molecular weight cutoff (Millipore). The RNA samples were dissolved in the final NMR buffer (10 mM sodium phosphate buffer (pH 6.5), 150 mM NaCl). Two uniformly 5F-Ura- and 5F-Cyt-labeled TAR RNA NMR samples were prepared with sample concentrations ranging from ∼1.0 to 1.2 mM in 500 μL of H_2O/D_2O (9:1).

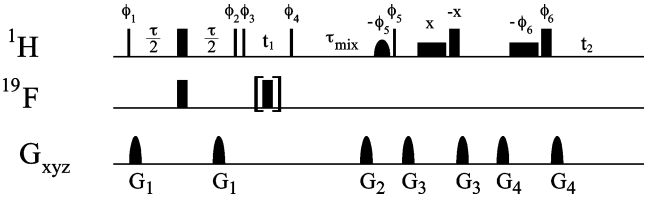

Figure 1. Pulse sequence for the S^{3}E-^{19}F-α,β-edited NOESY. Narrow and wide bars correspond to $\pi/2$ and π pulses, respectively, with phase along *x* unless indicated. High-power proton pulses were applied with a field strength of 25.8 kHz, while high-power ^{19}F pulses were applied with a field strength of 12.8 kHz. Water-selective Gaussian $\pi/2$ pulses ($-\phi_5$) of duration 8.0 ms using a $\gamma B_1/2\pi = 76$ Hz field strength was employed to achieve water flip-back.[45] Water suppression combined with minimal baseline distortion was achieved by excitation sculpting.[62] Water-selective square π pulses of duration 2.0 ms used a $\gamma B_1/2\pi = 250$ Hz field strength. The delay $\tau = 1/4J(H6,F) = 34.8$ ms. The NOESY mixing time, τ_{mix}, was 200 ms. Two spectra were recorded with (A): $\phi_1 = \pi/4, \pi/4, \phi_2 = 0, \pi/2, \phi_3 = 0, \pi/2, \phi_4 = 0, 0, \pi, \pi, \phi_5 = 4(0), 4(\pi), 4(\pi/2), 4(3\pi/2), \phi_6 = 4(0), 4(\pi/2)$, receiver $= 2(0, \pi, \pi, 0), 2(\pi/2, 3\pi/2, 3\pi/2, \pi/2)$; and (B): $\phi_1 = \pi/4, 5\pi/4, \phi_2 = 0, \pi/2, \phi_3 = \pi, 3\pi/2, \phi_4 = 0, 0, \pi, \pi, \phi_5 = 4(0), 4(\pi), 4(\pi/2), 4(3\pi/2), \phi_6 = 4(0), 4(\pi/2)$, receiver $= 2(0, \pi, \pi, 0), 2(\pi/2, 3\pi/2, 3\pi/2, \pi/2)$. Quadrature detection in the t_1 dimension was obtained by altering ϕ_4 according to States-TPPI.[63] Addition (A+B) and subtraction (A−B) of the interleaved experiments produced the two edited subspectra having a $\pi/2$ relative phase shift with ^{19}F adopting either β- or α-spin state.[10] Sine-shaped gradient durations and amplitudes were: $G_1 = 1$ ms (8.5 G/cm); $G_2 = 1$ ms (25 G/cm), $G_3 = 1$ ms (15.5 G/cm), and $G_4 = 1$ ms (5.5 G/cm). Directions: (*x*,*y*), *z*, (*x*,*y*,*z*), (*x*,*y*,*z*). ^{19}F refocusing during t_1 is optional, the bracketed π pulse was omitted in the present study.

NMR Spectroscopy. All NMR spectra were recorded at 600 MHz on a Bruker Avance spectrometer equipped with a 5 mm quadruple resonance (^{1}H, ^{19}F, ^{31}P, and ^{13}C-QXI) probe with shielded triple axis gradients at 25 °C. Carrier positions in the present work were −88.15 ppm for ^{19}F and 7.12 (HMBC) or 4.79 (S^{3}E-^{19}F-α,β-edited NOESY) ppm for^{1}H, respectively. All spectra were processed and analyzed using NMRPipe [21] and FELIX 2000 (MSI, San Diego, USA) program packages. For each phase-sensitive, gradient-selected HMBC experiment, 64 complex points were recorded with an acquisition time of 21.2 ms for ^{19}F (ω_1) and 1024 complex points with an acquisition time of 292.5 ms for ^{1}H (ω_2). A 1.3 s repetition delay between transients was used, with 128 scans per increment (total measuring time 8.5 h). The ω_2 dimension was apodized with a 126° shifted squared sinebell window function. Data sets were zero-filled twice before Fourier transformation. The ω_1 data were apodized with a 72° shifted squared sinebell window function and zero-filled prior to echo/antiecho Fourier transformation. The pulse sequence of Figure 1 was employed in recording the S^{3}E-^{19}F-α,β-edited NOESY data sets. For each S^{3}E-^{19}F-α,β-edited NOESY subspectrum, 512 complex points were recorded with an acquisition time of 96.7 ms for ^{1}H (ω_1) and 8192 complex

(7) Griesinger, C.; Sorensen, O. W.; Ernst, R. R. *J. Am. Chem. Soc.* **1985**, *107*, 6394−6396.
(8) Griesinger, C.; Sorensen, O. W.; Ernst, R. R. *J. Chem. Phys.* **1986**, *85*, 6837−6852.
(9) Griesinger, C.; Sorensen, O. W.; Ernst, R. R. *J. Magn. Reson.* **1987**, *75*, 474−492.
(10) Meissner, A.; Duus, J. O.; Sorensen, O. W. *J. Magn. Reson.* **1997**, *128*, 92−97.
(11) Meissner, A.; Duus, J. O.; Sorensen, O. W. *J. Biomol. NMR* **1997**, *10*, 89−94.
(12) Luy, B.; Marino, J. P. *J. Biomol. NMR* **2001**, *20*, 39−47.
(13) Luy, B.; Barchi, J. J., Jr.; Marino, J. P. *J. Magn. Reson.* **2001**, *152*, 179−184.
(14) Willker, W.; Leibfritz, D.; Kerssebaum, R.; Bermel, W. *Magn. Reson. Chem.* **1993**, *31*, 287−292.
(15) Cicero, D. O.; Barbato, G.; Bazzo, R. *J. Magn. Reson.* **2001**, *148*, 209−213.
(16) Metzler, W. J.; Leighton, P.; Lu, P. *J. Magn. Reson.* **1988**, *76*, 534−539.
(17) Collier, A. K.; Arnold, J. R. P.; Fisher, J. *Magn. Reson. Chem.* **1996**, *34*, 191−196.
(18) Seelamgari, A.; Maddukuri, A.; Berro, R.; de la Fuente, C.; Kehn, K.; Deng, L. W.; Dadgar, S.; Bottazzi, M. E.; Ghedin, E.; Pumfery, A.; Kashanchi, F. *Front Biosci.* **2004**, *9*, 2388−2413.
(19) Milligan, J. F.; Uhlenbeck, O. C. *Methods Enzymol.* **1989**, *180*, 51−62.
(20) Scott, L. G.; Geierstanger, B. H.; Williamson, J. R.; Hennig, M. *J. Am. Chem. Soc.* **2004**, *126*, 11776−11777.
(21) Delaglio, F.; Grzesiek, S.; Vuister, G. W.; Zhu, G.; Pfeifer, J.; Bax, A. *J. Biomol. NMR* **1995**, *6*, 277−293.

points with an acquisition time of 619.3 ms for ^1H (ω_2). A repetition delay of 1.2 s was used between transients, with 48 scans per increment (total measuring time 18.5 h). A solvent suppression filter was used in the ω_2 dimension to eliminate distortions from residual water prior to applying a Lorentz-to-Gauss window function. Data sets were zero-filled twice before Fourier transformation. The ω_1 data were apodized with a 72° shifted squared sinebell window function and zero-filled prior to Fourier transformation. The absorptive part of the final 2D matrices were 2048 × 128 points for the two HMBC experiments (recorded on 5F-Ura- and 5F-Cyt-substituted TAR) and 16 384 × 2048 points for each subspectrum of the two S^3E-^{19}F-α,β-edited NOESY experiments, respectively.

Density Functional Theory Calculations. Theoretical generalized Karplus relations for ^5J(H1′,F) couplings as a function of the glycosidic torsion angle χ have been determined for 5F-Cyt and 5F-Ura ribonucleosides. Molecular geometries have been optimized in Kohn−Sham calculations with the B3LYP functional[22,23] and the 6-31G(d) basis[24,25] in the implementation of Gaussian 98.[26] The values of the backbone torsion angles β, γ, δ, and ϵ were frozen to their mean values in canonical A-form RNA: (β) 178°, (γ) 54°, (δ) 82°, (ϵ) 207°.[27] The glycosidic torsion angle χ was constrained to its target value, 0−360°, in 30° increments. All other structural parameters have been optimized. For each nucleoside, two sets of optimizations have been performed corresponding to C3′-endo (*north*) pucker and C2′-endo (*south*) sugar conformation normally associated with A-form and B-form geometry, respectively. The latter calculations were performed with backbone torsion angles β, γ, δ, and ϵ frozen to their mean values in canonical B-form DNA.[27] The computed structures are provided as Supporting Information.

Spin−spin coupling constants were calculated by a combined Sum-Over-States density functional perturbation theory (SOS-DFPT; for the paramagnetic and diamagnetic spin−orbit terms [PSO and DSO], respectively) and DFT/finite perturbation theory (FPT; for the Fermi-Contact [FC] term) approach as implemented in the deMon NMR code.[5,28,29] The spin-dipolar (SD) term has been neglected in the present approach for the following reasons: (a) this term is usually relatively small for longer-range coupling; (b) it is in most cases smaller than the error in the DFT calculation of the FC term; and (c) it represents the most time-consuming step of nuclear spin−spin coupling calculations at the DFT level.[5,28,29] The density functional calculations employed Perdew and Wang's generalized gradient approximation (GGA) for exchange[30] in combination with Perdew's GGA for correlation (PWP86).[31,32] Although hybrid functionals, such as B3LYP, seem best for spin−spin coupling calculations,[33] the PWP86 GGA provides similar results for the absolute value of the FC term and especially for its structural trends.[34] The basis set IGLO-III of Kutzelnigg et al.[35] was used for all atoms. The H1′ atom has been chosen as the center of the finite perturbation with the perturbation parameter $\lambda = 0.001$.

Results and Discussion

Measurement of Long-Range ^5J(H1′,F) Couplings. The proliferation of RNA structure determinations using NMR spectroscopy is in part attributable to established methods for isotopic labeling of RNA molecules with ^{13}C and ^{15}N.[36,37] An alternative economical approach to conventional ^{13}C and ^{15}N isotopic labeling is to label with a nonnatural nucleus, such as ^{19}F, that affords 100% natural abundance, high sensitivity, and large chemical shift dispersion. The specific labeling of RNA with ^{19}F at the 2′-position in the ribose can be problematic especially for regions adopting noncanonical conformations because of the conformational bias imposed by the fluorine substitution. 2′-Deoxy-2′-fluorinated nucleosides are effectively locked in the C3′-endo sugar pucker normally associated with A-form RNA geometry.[38−40] In contrast, 5-fluorouridine substitutions do not perturb the structure of tRNA.[41] Additionally, resolved ribose H1′ protons in 5-fluoropyrimidine-substituted TAR RNA do not experience large chemical shift changes with respect to unmodified TAR RNA, suggesting a very similar local environment. Thus, the introduction of ^{19}F substitutions into the heterocyclic bases of RNA oligonucleotides is generally nonperturbing and provides us with uniquely positioned, sensitive reporter groups for NMR structural and dynamical studies.

For assignment of the F5 resonances in 5-fluoropyrimidine-substituted TAR, we recorded proton-detected HMBC experiments shown in Figure 2. In addition to the expected H6−F5 cross-peaks (^3J(H6,F) coupling ∼7 Hz), we observed a long-range scalar ^5J(H1′,F) coupling, which had been previously observed in fluorinated pyrimidine nucleosides.[3,4] Remarkably, besides the expected correlations due to conformationally independent vicinal connecting base F5 and H6 resonances, all but one modified residue (U31) in 5F-Cyt- and 5F-Ura-substituted TAR show cross-peaks to their respective ribose H1′ resonances (Figure 2). Such intraresidual long-range ^5J(H1′,H5) couplings were also observed in unmodified pyrimidine nucleosides[42] and small oligoribonucleotides.[43,44] Establishing unambiguous base F5 and anomeric H1′ connectivities during the assignment procedure proved to be extremely useful in that these identify correlations to resolved ribose protons that do not experience large chemical shift changes due to close proximity to the fluorine substituent. Shielding or deshielding effects due to the presence of the fluorine can be studied by comparing chemical shifts of protons in unmodified TAR and 5-fluoropyrimidine-substituted TAR. The influence of a fluorine substitution on chemical shifts of protons is expected to be strongest if these protons are in close proximity to the fluorine

(22) Becke, A. D. *Phys. Rev. A* **1988**, *38*, 3098−3100.
(23) Becke, A. D. *J. Chem. Phys.* **1993**, *98*, 5648−5652.
(24) Frisch, M. J.; Pople, J. A.; Binkley, J. S. *J. Chem. Phys.* **1984**, *80*, 3265−3269.
(25) Hehre, W. J.; Ditchfie, R.; Pople, J. A. *J. Chem. Phys.* **1972**, *56*, 2257−2261.
(26) Frisch, M. J.; et al. *Gaussian 98*; Gaussian, Inc.: Pittsburgh, PA, 1998.
(27) Saenger, W. *Principles of Nucleic Acid Structure*; Springer-Verlag: New York, 1984.
(28) Salahub, D. R.; Fournier, R.; Mlynarski, P.; Papai, I.; St. Amant, A.; Ushio, J. In *Density Functional Methods in Chemistry*; Labanowski, J. K., Andzelm, J., Eds.; Springer-Verlag: New York, 1991; pp xv, 443.
(29) Malkin, V. G.; Malkina, O. L.; Casida, M. E.; Salahub, D. R. *J. Am. Chem. Soc.* **1994**, *116*, 5898−5908.
(30) Perdew, J. P.; Yue, W. *Phys. Rev. B* **1986**, *33*, 8800−8802.
(31) Perdew, J. P. *Phys. Rev. B* **1986**, *33*, 8822−8824.
(32) Perdew, J. P. *Phys. Rev. B* **1986**, *34*, 7406.
(33) Helgaker, T.; Pecul, M. In *Calculation of NMR and EPR Parameters*; Kaupp, M., Buehl, M., Malkin, V. G., Eds.; Wiley-VCH: Weinheim, Germany, 2004; pp 101−121.
(34) Munzarová, M. L. In *Calculation of NMR and EPR Parameters*; Kaupp, M., Buehl, M., Malkin, V. G., Eds.; Wiley-VCH: Weinheim, Germany, 2004; pp 463−482.
(35) Kutzelnigg, W.; Fleischer, U.; Schindler, M. *NMR: Basic Principles and Progress*; Springer-Verlag: New York, 1990; Vol. 23, p 165.
(36) Nikonowicz, E. P.; Sirr, A.; Legault, P.; Jucker, F. M.; Baer, L. M.; Pardi, A. *Nucleic Acids Res.* **1992**, *20*, 4507−4513.
(37) Batey, R. T.; Inada, M.; Kujawinski, E.; Puglisi, J. D.; Williamson, J. R. *Nucleic Acids Res.* **1992**, *20*, 4515−4523.
(38) Thibaudeau, C.; Plavec, J.; Chattopadhyaya, J. *J. Org. Chem.* **1998**, *63*, 4967−4984.
(39) Barchi, J. J., Jr.; Jeong, L. S.; Siddiqui, M. A.; Marquez, V. E. *J. Biochem. Biophys. Methods* **1997**, *34*, 11−29.
(40) Reif, B.; Wittmann, V.; Schwalbe, H.; Griesinger, C.; Worner, K.; Jahn-Hofmann, K.; Engels, J. W.; Bermel, W. *Helv Chim. Acta* **1997**, *80*, 1952−1971.
(41) Chu, W. C.; Horowitz, J. *Nucleic Acids Res.* **1989**, *17*, 7241−7252.
(42) Hruska, F. E. *Can. J. Chem.* **1971**, *49*, 2111−2118.
(43) Bain, A. D.; Bell, R. A.; Everett, J. R.; Hughes, D. W. *Can. J. Chem.* **1980**, *58*, 1947−1956.
(44) Orban, J.; Bell, R. A. *J. Biomol. Struct. Dyn.* **1990**, *7*, 837−848.

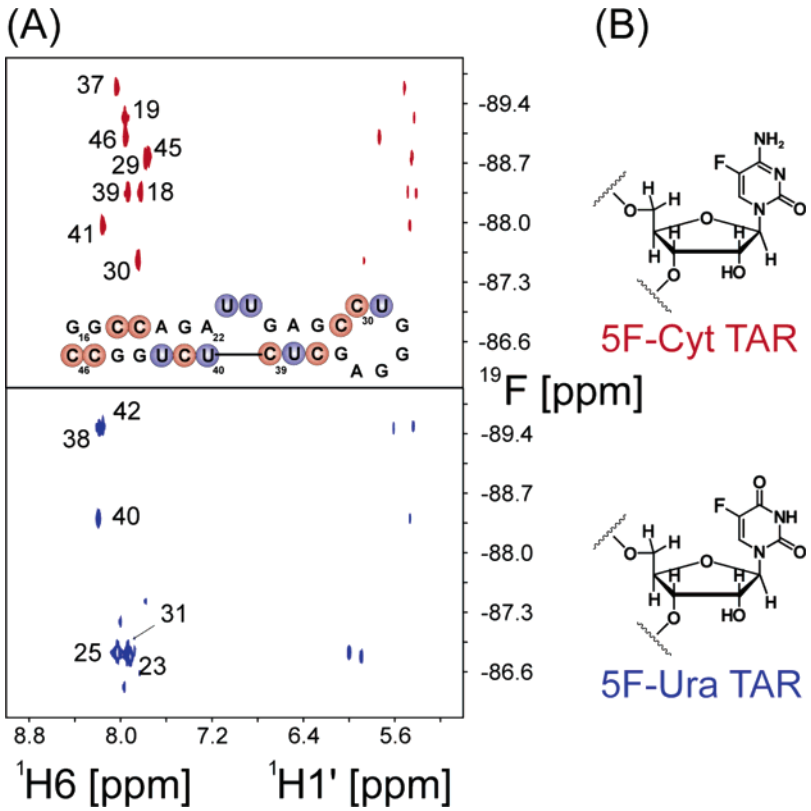

Figure 2. (A) Phase-sensitive $^{1}H,^{19}F$ HMBC spectra of 5F-Cyt- and 5F-Ura-substituted TAR. The delay for $^{1}H-^{19}F$ coupling evolution was set to 80 ms, three gradients with gradient ratios $G_1:G_2:G_3 = 1:-1:1.88$ (odd experiments) and $-1:1:1.88$ (even experiments) were employed for echo-antiecho quadrature detection.[14,15] Near absorption profiles in ω_1 were obtained prior to magnitude calculation in ω_2. Assignments of individual HMBC cross-peaks between ^{19}F nuclei and base H6 protons are given. The inset shows the sequence and secondary structural representation of HIV-2 TAR with 5F-Cyt (red) and 5F-Ura (blue) substitutions. (B) Chemical structures of modified 5-fluorouridine and 5-fluorocytidine nucleosides.

Table 1. Glycosidic Torsion Angles χ, Experimental and Calculated $^{5}J(H1',F)$ Couplings, H1′ and H6 Chemical Shifts for 5F-Pyrimidine-Substituted TAR, and Differences in Chemical Shifts between Modified and Unmodified RNA

nucleotide	χ (deg)[a]	$^{5}J(H1',F)$ (Hz) (expt)	$^{5}J(H1',F)$[b] (Hz) (calcd)	$\delta(^{1}H1')$[c] (ppm)	$\delta(^{1}H6)$ (ppm)	$\Delta\delta(^{1}H1')$[d] (ppm)	$\Delta\delta(^{1}H6)$ (ppm)
C18	222	0.3	3.1	5.49	7.82	−0.08	0.10
C19	202	0.6	2.3	5.43	7.96	−0.06	0.23
U23	237	1.0	3.5	5.89	7.92	0.00	0.21
U25	276	1.0	3.3	6.00	8.03	0.05	0.13
C29	205	0.3	2.5	5.46	7.78	−0.06	0.22
C30	266	nd[e]	3.5	5.87	7.85	−0.03	0.18
U31	240	nd[e]	3.5	5.77	7.94	0.02	0.17
C37	224	0.8	3.2	5.56	8.04	−0.02	0.23
U38	208	1.1	2.6	5.61	8.19	−0.01	0.29
C39	200	0.4	2.3	5.42	7.94	−0.07	0.23
U40	172	1.1	1.1	5.54	8.20	0.01	0.28
C41	208	0.7	2.6	5.51	8.16	0.00	0.21
U42	201	1.0	1.8	5.44	8.16	−0.06	0.27
C45	204	0.4	2.4	5.45	7.76	−0.08	0.11
C46	231	1.2	3.3	5.74	7.96	−0.06	0.26

[a] Reference glycosidic torsion angles χ were extracted from the NMR structure of unmodified TAR RNA (unpublished results). Glycosidic torsion angles were restrained to $\chi = 194 \pm 30°$ during simulated annealing for nucleotides in A-form helical regions (bulged residues U23 and U25 as well as loop residues C30 and U31 were not restrained). [b] The calculated $^{5}J(H1',F)$ couplings were obtained using the χ torsion angles given in column 1 together with the theoretical Karplus parameters for C3′-endo sugar conformations (Table 2). [c] ^{1}H chemical shifts were externally referenced to DSS, with ^{19}F chemical shifts referenced indirectly according to $^{19}F/^{1}H$ (TFA in a sphere)[61] chemical shift ratios in DSS. [d] Chemical shift changes $\Delta\delta$ ($\Delta\delta$[ppm] = $\delta_{5F-pyrimidine-TAR}$[ppm] − δ_{wt-TAR}[ppm]) of base H6 and anomeric H1′ proton resonances induced by the 5F-pyrimidine substitutions. [e] Insufficiently resolved for accurate measurement.

atom (e.g., for the base H6 protons). The chemical shift data shown in Table 1 reveal that all base H6 protons are deshielded ($\Delta\delta_{average}(H6) = 0.21 \pm 0.06$ ppm) as a consequence of the strongly electron-withdrawing nature of the fluorine substituent. There is essentially no chemical shift effect for the anomeric H1′ protons ($\Delta\delta_{average}(H1') = -0.03 \pm 0.04$ ppm).

It should be emphasized that the proton-detected $^{1}H,^{19}F$ HMBC experiment provides a valuable and sensitive alternative to heteronuclear NOE (HOESY) approaches for generating two-dimensional H6,F correlations that render overlaps in one-dimensional ^{19}F spectra (Figure 2A). In particular, through-bond HMBC correlations seem advantageous in the context of probe technology optimized for ^{1}H detection. High-quality $^{1}H,^{19}F$ HMBC experiments tailored for the detection of H6,F correlations (with the delay for $^{1}H-^{19}F$ long-range coupling evolution set to ∼60−80 ms) can be recorded in about 2 h on ∼1.0 mM

TAR RNA samples. However, we were not able to observe HMBC cross-peaks connecting the base F5 nuclei and exchangeable protons such as the imino H3 of 5-fluorouridine or amino H41/H42 protons of 5-fluorocytidine in modified TAR RNA, presumably due to effects of exchange.

The accurate measurement of the small ^5J(H1′,F) coupling interactions is critical to permit interpretation in the context of nucleic acid conformations. The separation of the two doublet components of an E. COSY-type cross-peak provides a convenient approach to measure small couplings and eliminates the potential increase in overlap associated with doublets generated by standard E. COSY techniques. We have chosen a ^{1}H,^{19}F-S^{3}E pulse sequence element in order to exclusively excite the base H6 proton resonances in 5-fluoropyrimidine-substituted TAR with the F5 nuclei in either the α- or β-spin state.[13] The theory behind the S^{3}E concept has been described in great detail.[10,11] Briefly, the S^{3}E element at the beginning of the S^{3}E-^{19}F-α,β-edited NOESY experiment shown in Figure 1 allows for ^3J(H6,F) coupling evolution, and subsequent phase cycling selects either F$^\alpha$ or F$^\beta$ spin states. Two experiments are recorded in an interleaved manner, and post-acquisition addition and subtraction creates the edited subspectra (see Figure legend 1 for details). The S^{3}E editing scheme is concatenated with a homonuclear water-flip back NOESY sequence to transfer magnetization among base and ribose proton spins.[45] If the ^{19}F spins are left unperturbed during the indirect t_1 and the detected proton evolution time t_2, cross-peaks in the edited subspectra experience displacements due to both the ^3J(H6,F) and ^5J(H1′,F) coupling interactions. Optionally, the passive ^3J(H6,F) couplings can be suppressed by means of refocusing during t_1 so that the submultiplets appear centered at the chemical shift of the base H6 protons. Given the relatively small magnitude of the passive ^3J(H6,F) couplings utilized in the editing process, the S^{3}E element offers the highest sensitivity combined with similar accuracy compared to alternative approaches employing α/β half-filters, where editing filter delays are tuned to 1/2J as opposed to 1/4J.[46,47]

Homonuclear NOESY mixing schemes efficiently transfer magnetization from base to ribose protons generating cross-peaks from either intraresidual (H1′$_i$,H6$_i$) or sequential interresidual (H1′$_{i+1}$,H6$_i$) correlations (Figure 3). The NOESY mixing time is chosen (τ_{mix} = 200 ms) such that cross-peak intensities are near their maximum. Only anomeric H1′$_i$ protons belonging to the same residue participate in the system of three mutually coupled spins together with base H6$_i$ protons and F5$_i$, thus only intraresidual (H1′$_i$,H6$_i$) cross-peaks show a displacement in ω_2 due to the long-range ^5J(H1′,F) couplings, as shown in Figure 3. The apparent long-range J-couplings can easily be measured by taking appropriate 1D traces of the individual subspectra corresponding to either F$^\alpha$ or F$^\beta$ spin states, displacing the two extracted ω_2 rows with respect to each other, and forming the integral of the power difference spectrum as a function of the displacement.[48] The estimated precision is about ±0.1 Hz and limited by the digital resolution of zero-filled 1D traces. We note, however, that the described S^{3}E-^{19}F-α,β-edited NOESY

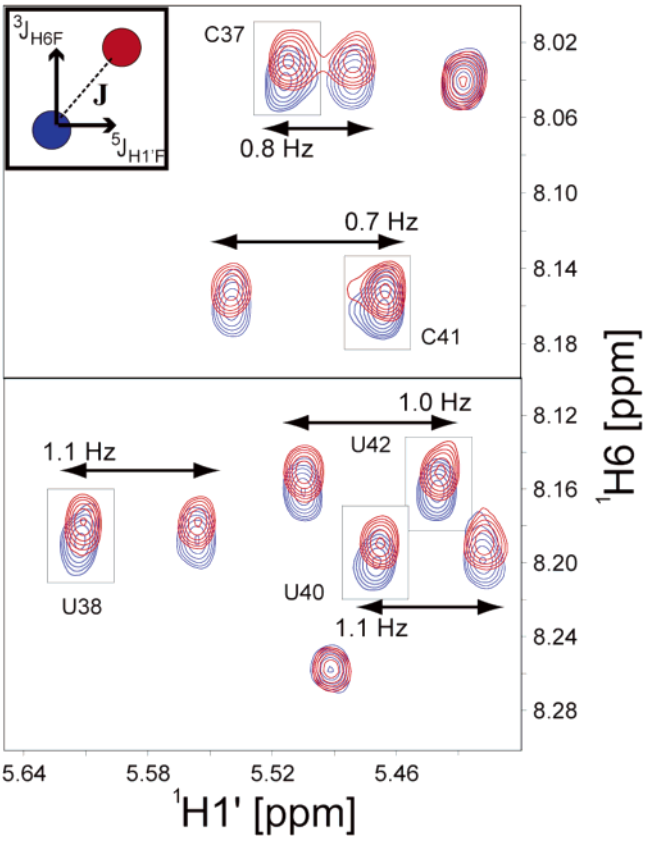

Figure 3. S^{3}E-^{19}F-α,β-edited NOESY experiment for 5F-Cyt- and 5F-Ura-substituted TAR. Individual subspectra shown in blue and red are superimposed and correspond to the passive ^{19}F spins adopting β- and α-states, respectively. Assigned NOE cross-peaks stem from either intraresidual (H1′$_i$,H6$_i$) or sequential interresidual (H1′$_{i+1}$,H6$_i$) correlations. Extracted ^5J(H1′,F) couplings are reported. Only intraresidual (H1′$_i$,H6$_i$) cross-peaks (gray boxes) show a displacement in ω_2 due to ^5J(H1′,F) couplings. Remaining centered cross-peaks are from unmodified residues not exhibiting splitting due to ^3J(H6,F) couplings. The inset shows a schematic superposition of the two subspectra (H1′$_i$,H6$_i$ cross-peak) with the ^{19}F spin in either α- (red) or β- (blue) state. The displacement vector **J** between the submultiplets consists of the ^3J(H6,F) coupling in ω_1 and the ^5J(H1′,F) coupling in ω_2.

is susceptible to differential relaxation effects.[49,50] We have not attempted to correct for finite ^{19}F T_1 relaxation times, which leads to a systematic decrease of the reported apparent long-range J-couplings.[51] However, corrections should be very small given the long (nonselective) inversion recovery times ($T_1 \approx$ 930 ms) of resolved ^{19}F resonances in 5-fluorouridine-substituted TAR measured at 564.6 MHz. Errors stemming from J-mismatches (i.e., differences between the actual ^3J(H6,F) coupling values from the ones used to calculate the S^{3}E filter delay) can safely be neglected.

The employed E. COSY-type experiments allow for the determination of relative signs of scalar J-coupling interactions. The uniformly positive tilt of the **J** displacement vector in Figure 3 indicates identical signs of ^3J(H6,F) and ^5J(H1′,F) coupling interactions (the proton and fluorine gyromagnetic ratios, γ_H and γ_F, have the same sign). The vicinal ^3J(H6,F) coupling can be assumed to be positive,[38] hence, the measured long-range ^5J(H1′,F) couplings are likewise positive. The observed long-

(45) Lippens, G.; Dhalluin, C.; Wieruszeski, J. M. *J. Biomol. NMR* **1995**, *5*, 327−331.
(46) Ottiger, M.; Delaglio, F.; Bax, A. *J. Magn. Reson.* **1998**, *131*, 373−378.
(47) Andersson, P.; Weigelt, J.; Otting, G. *J. Biomol. NMR* **1998**, *12*, 435−441.
(48) Schwalbe, H.; Rexroth, A.; Eggenberger, U.; Geppert, T.; Griesinger, C. *J. Am. Chem. Soc.* **1993**, *115*, 7878−7879.
(49) Norwood, T. J.; Jones, K. *J. Magn. Reson., Ser. A* **1993**, *104*, 106−110.
(50) Harbison, G. S. *J. Am. Chem. Soc.* **1993**, *115*, 3026−3027.
(51) Rexroth, A.; Schmidt, P.; Szalma, S.; Geppert, T.; Schwalbe, H.; Griesinger, C. *J. Am. Chem. Soc.* **1995**, *117*, 10389−10390.

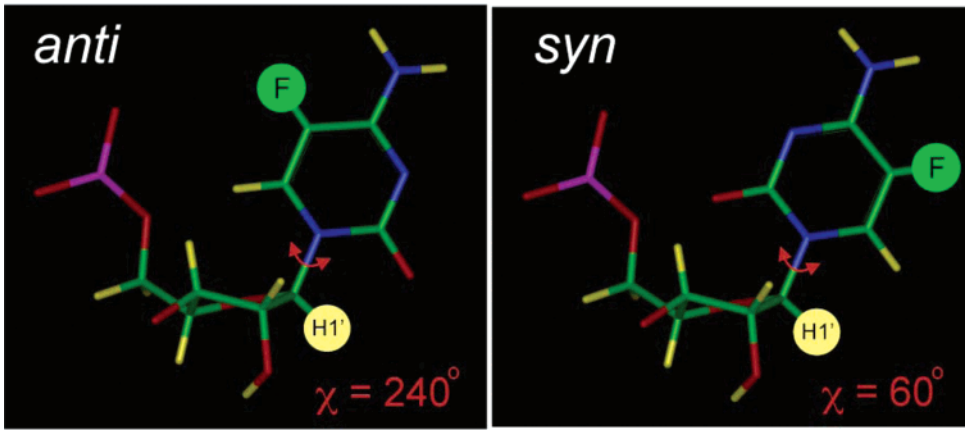

Figure 4. The *anti* ($\chi \approx 240°$) and *syn* ($\chi \approx 60°$) conformations of the glycosidic torsion angle χ (O4′−C1′−N1−C2) in 5F-Cyt. Long-range ^5J(H1′,F5)-coupled nuclei F5 and H1′ are highlighted.

range ^5J(H1′,F) couplings in 5-fluorouridine- or 5-fluorocytidine-substituted TAR RNA are invariably small and range from 0.3 (observed for residues C18 and C29) to 1.2 (C46) Hz (Table 1). Scalar ^5J(H1′,F) couplings previously reported in the literature range from 1.0 to 1.8 Hz as measured for various fluorinated nucleoside analogues.[3,4] We obtain ^5J(H1′,F) couplings of 1.5 Hz from the (selectively H2′ decoupled) H1′ doublets of 5-fluorouridine and 5-fluorocytidine nucleosides in methanol at 20 °C. There appears to be little systematic difference in the magnitude of the ^5J(H1′,F) coupling interactions on going from 5-fluorouridine to 5-fluorocytidine in the TAR RNA.

Calculation of the Glycosidic Torsion Dependence of ^5J(H1′,F). The glycosidic torsion angle χ (O4′−C1′−N1−C2 in pyrimidine and O4′−C1′−N9−C4 in purine nucleosides, respectively), which defines the orientation of the nucleobase with respect to the attached sugar in nucleic acids, is sterically restricted to either the *syn* ($\chi \approx 60°$) or *anti* ($\chi \approx 240°$) conformation. In the case of pyrimidine ribonucleosides with C3′-endo sugar pucker, the *anti* conformation greatly dominates as a consequence of unfavorable steric interactions between the 2-keto oxygen and the endo ribose substituents.[27] The *anti* conformation for the glycosidic torsion angle χ rotates the C1′−H1′ bond such that it approaches an orientation coplanar with the base plane so that an extended "W" (*trans*−*trans*) configuration connects the fluorine nucleus covalently bound to the base C5 carbon and the anomeric H1′ proton in 5-fluoropyrimidine-substituted RNA, as shown in Figure 4. This extended W configuration is most suited for long-range couplings to occur in unsaturated systems. The absence of observable long-range ^5J(H1′,H5) scalar couplings in orotidine (6-carboxyuridine) can be explained on the basis of altered preferences for the *syn* conformation of the glycosidic torsion angle χ disrupting the extended W configuration.[42]

NMR parameters including spin−spin coupling constants of small molecular systems can be calculated by a number of methods, such as coupled-cluster theory involving triple excitation operators. Unfortunately, the high computational cost typically limits the applicability of these methods to systems involving very few atoms. At present, the only methods capable of treating polyatomic systems of the size of 5-fluorouridine and 5-fluorocytidine using reasonable computational resources are those provided by DFT.[33] The accurate calculation of spin−spin coupling constants involving electron-rich atoms, such as fluorine, still represents a challenge for the currently used exchange-correlation functionals.[5,33,52] In particular, the quality of the DFT description of the FC contribution deteriorates with increasing number of lone pairs on the coupled atoms. However, semiquantitative to good agreement with experiment has been obtained for four-bond ^4J(F,F) couplings in fluorinated naphthalenes[53] and for three- to seven-bond couplings in fluorinated pyridines.[6] These studies have relied upon the dominant contribution of the PSO term to the overall coupling constant. On the other hand, the long-range ^5J(H1′,F5) scalar couplings in 5-fluoropyrimidine nucleosides are dominated by the more challenging FC term. Under these circumstances, large disagreements between experimental values and DFT values are frequently observed; examples of this behavior are ^1J(H,F) coupling constants of HF and $[FHF]^-$ which are significantly underestimated by DFT.[33] The adequate description of the spin polarization of the core shells seemingly constitutes the most difficult problem for DFT calculations aiming to reproduce the magnitude of the FC term. However, trends in structural parameters implicate trends in the spin distribution within the valence shells that are usually well reproduced by DFT-based methods.[54] This ability of DFT to reproduce trends in the FC term is well documented for a wide range of density functionals even if the calculation fails to determine its exact magnitude.[34,55] We subsequently show that the ^5J(H1′,F5) spin−spin couplings studied here qualitatively follow a Karplus-like dependence with the torsion angle χ, although we note a discrepancy between absolute calculated and experimental *J*-coupling values.

The ab initio values together with experimentally measured ^5J(H1′,F5) couplings are plotted in Figure 5. The four computed data sets (blue triangles and red dots and squares in Figure 5) have been fitted to the Karplus-type function $y = A\cdot\cos^2(x - D) + B\cdot\cos(x - D) + C$, with parameters reported in Table 2, and correlation coefficients ranging from 0.990 to 0.996. The theoretical couplings reveal a shallow minimum (especially for 5F-Cyt) for the *syn* ($\chi \approx 60°$) and a steeper maximum for the *anti* ($\chi \approx 240°$) glycosidic torsion angle conformation, in agreement with the exceptional suitability of the extended W configuration for long-range coupling (Figure 4). Interestingly,

(52) Lantto, P.; Vaara, J.; Helgaker, T. *J. Chem. Phys*. **2002**, *117*, 5998−6009.
(53) Peralta, J. E.; Barone, V.; Contreras, R. H.; Zaccari, D. G.; Snyder, J. P. *J. Am. Chem. Soc*. **2001**, *123*, 9162−9163.
(54) Munzarová, M. L.; Kubacek, P.; Kaupp, M. *J. Am. Chem. Soc.* **2000**, *122*, 11900−11913.
(55) Munzarová, M.; Kaupp, M. *J. Phys. Chem. A* **1999**, *103*, 9966−9983.

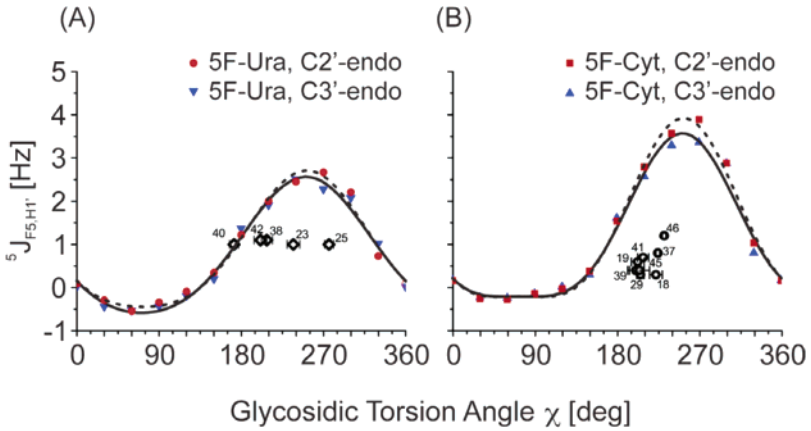

Figure 5. Experimental ^{5}J(H1′,F) couplings as a function of glycosidic torsion angle χ for (A) 5F-Ura- and (B) 5F-Cyt-substituted TAR (open diamonds; summarized in Table 1); χ torsion angle errors corresponding to the range observed within the 20 lowest energy NMR structures (unpublished results). Theoretical Karplus relations were obtained for (A) isolated 5-fluorouridine with C3′-endo pucker (solid line, blue triangles) and C2′-endo pucker (dashed line, red dots) and (B) isolated 5-fluorocytidine nucleosides with C3′-endo (solid line, blue triangles) pucker and C2′-endo (dashed line, red squares) sugar conformations, respectively.

Table 2. Theoretical Karplus Parameters ($y = A\cdot\cos^2(x - D) + B\cdot\cos(x - D) + C$) for ^{5}J(H1′,F) Couplings in 5-Fluorouridine and 5-Fluorocytidine Nucleosides

nucleoside	*A* (Hz)	*B* (Hz)	*C* (Hz)	*D* (deg)
5F-Cyt, *north*[a]	0.98	−1.89	0.72	71.97
5F-Cyt, *south*	1.14	−2.06	0.73	72.97
5F-Ura, *north*	0.37	−1.57	0.62	70.98
5F-Ura, *south*	0.53	−1.58	0.60	71.81

[a] C3′-endo (*north*) pucker and C2′-endo (*south*) sugar conformations are normally associated with A-form and B-form geometry, respectively.

the calculated Karplus-type relations predict a sign change for the *syn* with respect to the *anti* conformation. Obviously, the long-range five-bond ^{5}J(H1′,F5) couplings follow the same type of functional dependence on the glycosidic torsion angle χ as do the vicinal three-bond ^{3}J(H1′,C2) and ^{3}J(H1′,C6) and the one-bond ^{1}J(H1′,C1′) couplings.[56] This observation suggests a similar mechanism governing the transfers of spin density from H1′ toward F5 over one, three, and five bonds, respectively. The existence of one minimum and one maximum for the five-bond coupling, as opposed to two minima and two maxima for the three-bond couplings, manifests itself in a distinct ratio for the coefficients *A* and *B* corresponding to the quadratic and linear cosine terms, respectively. The Karplus relation is dominated by the quadratic (2 maxima) cosine term for the three-bond couplings,[56] whereas the linear (1 maximum) cosine term dictates the five-bond couplings (see Table 2). A comparison of the four computed curves in Figure 5 reveals that the magnitude of the ^{5}J(H1′,F) interactions exhibits a strong dependence on the type of the nucleoside involved, that is, 5-fluorouridine or 5-fluorocytidine. In contrast, the influence of the sugar pucker appears to be negligible. This is understandable considering that four out of the five bonds involved in the coupling pathway belong to the aromatic ring system of the nucleobase, associated with distinctly different electron distributions for 5-fluorouridine and 5-fluorocytidine. The conformational environment of C1′ is expected to only marginally influence the electron distribution within the coupling pathway.

Figure 5 reveals that theoretical ^{5}J(H1′,F) couplings obtained for isolated ribonucleosides are overestimated with respect to the experimental values for the oligonucleotide in solution. In the case of 5F-Ura, a much closer agreement between experiment and ab initio calculated couplings is found for the canonical, base-paired nucleotides U38, U40, and U42 with respect to the noncanonical, bulge residues U23 and U25. It should be noted that the free TAR bulge exhibits increased flexibility compared to the more rigid, flanking A-form helices in the upper and lower stem regions.[57] The relatively tight ranges observed for the χ torsion angle as sampled by the 20 lowest energy NMR structures may not reflect the bulge dynamics properly (unpublished results). For 5F-Cyt, where all nucleotides but C30 are engaged in canonical base pairs in TAR, the theoretical ^{5}J(H1′,F) couplings seem to be significantly overestimated. However, with the exception of C18, for which the experimental ^{5}J(H1′,F) value is only 0.3 Hz, the remaining 5F-Cyt residues show increasing H−F spin−spin couplings for larger glycosidic torsion angles. The experimental ^{5}J(H1′,F) couplings range from 0.3 to 0.7 Hz for $\chi < 210°$ and reach 1.2 Hz for $\chi > 210°$. Base-pairing interactions are known to have a pronounced influence on spin−spin *J*-couplings within the aromatic bases,[58] and furthermore, the fluorine atom is expected to participate in F···H−O interactions with the solvent in the major groove of the RNA.[59] Thus, we largely attribute the disagreement between experiment and theory to leaving those dielectric solvent effects unaccounted for in the in vacuo quantum chemical calculations.

All pyrimidine residues in unmodified TAR adopt the *anti* conformation around the glycosidic torsion angle χ (Table 1). Thus, our present study is in agreement with unaltered preferences around the glycosidic torsion angle χ for 5-fluoropyrimidine nucleosides[3] and restricts χ of 5-fluorouridines and 5-fluorocytidines in 5-fluoropyrimidine-substituted TAR to the preferred *anti* conformer. The interpretation of the mechanism of long-range interactions involving ^{19}F nuclei remains controversial. Through-space mechanisms involving 2p−lone pair orbital overlap have been proposed for systems where the fluorine and a coupled proton are spatially proximate and the

(56) Munzarová, M. L.; Sklenář, V. *J. Am. Chem. Soc.* **2003**, *125*, 3649−3658.
(57) Dayie, K. T.; Brodsky, A. S.; Williamson, J. R. *J. Mol. Biol.* **2002**, *317*, 263−278.
(58) Fiala, R.; Munzarová, M. L.; Sklenář, V. *J. Biomol. NMR* **2004**, *29*, 477−490.
(59) Arnold, J. R. P.; Fisher, J. *J. Magn. Reson.* **2000**, *142*, 1−10.

sum of the van der Waals radii does not exceed ~2.6 Å.[39,60] In the present study, the extended W configuration of the H1′−C1′−N1−C6−C5−F5 bond network maximizes the distance between the coupled nuclei (>5 Å), suggesting that the electronic factors governing the five-bond interaction in 5-fluoropyrimidines are through-bond rather than through-space.

Conclusions

The intraresidual ^5J(H1′,F) coupling can successfully be used to correlate modified 5-fluoropyrimidine bases and the ribose to facilitate NMR resonance assignments. Standard through-bond gradient-selected HMBC experiments can be employed to correlate base F5 nuclei and anomeric H1′ protons in a more sensitive manner compared to through-space HOESY approaches. Although ^5J(H1′,F) couplings were previously observed for modified nucleosides,[3,4] they have not been observed or exploited in the assignment process of a folded RNA molecule of medium size. The phenomenon can be qualitatively explained on the basis of an extended W configuration of the H1′−C1′−N1−C6−C5−F5 bond network, which restricts the intervening glycosidic torsion angle χ of 5-fluorouridines and 5-fluorocytidines in 5-fluoropyrimidine-substituted TAR to the preferred *anti* conformer. The employed DFT approach provides an adequate description of the torsion angle dependence of the spin−spin coupling constants and reveals a Karplus-type dependence of ^5J(H1′,F) couplings with respect to the intervening torsion angle χ. The observed χ dependences of ^5J(H1′,F) show pronounced variations for 5F-Ura and 5F-Cyt 5-fluoropyrimidine nucleosides. The effect of sugar pucker variations on the scalar couplings is negligible, suggesting that the presented Karplus relations can be applied to RNA and DNA. We applied a S^3E-^{19}F-α,β-edited NOESY experiment that readily allows for the measurement of magnitude and signs of the small long-range intraresidual ^5J(H1′,F) couplings in a macromolecule.

Acknowledgment. The authors thank Edit Sperling for help in preparing the fluorinated triphosphates, and Olga L. Malkina for helpful discussions. This work was supported by The Skaggs Institute for Chemical Biology (J.R.W.), the National Institutes of Health (F32 CA80349 to L.G.S., GM-53320 to J.R.W., and GM-66669 to M.H.), and by the Grant MSM0021622413 of the Ministry of Education of the Czech Republic (M.M. and V.S.).

Supporting Information Available: Complete citation for ref 26 and optimized 5F-Cyt and 5F-Ura ribonucleoside structures used to compute the torsion angle dependence of the ^5J(H1′,F) spin−spin coupling constants. This material is available free of charge via the Internet at http://pubs.acs.org.

JA060165T

(60) Mallory, F. B.; Luzik, E. D.; Mallory, C. W.; Carroll, P. J. *J. Org. Chem.* **1992**, *57*, 366−370.
(61) Maurer, T.; Kalbitzer, H. R. *J. Magn. Reson., Ser. B* **1996**, *113*, 177−178.
(62) Hwang, T. L.; Shaka, A. J. *J. Magn. Reson., Ser. A* **1995**, *112*, 275−279.
(63) Marion, D.; Ikura, M.; Tschudin, R.; Bax, A. *J. Magn. Reson.* **1989**, *85*, 393−399.